

ORIGINAL ARTICLE

Evaluation of pulmonary disease using static lung volumes in primary ciliary dyskinesia

Massimo Pifferi,¹ Andrew Bush,² Giovanni Pioggia,³ Davide Caramella,⁴ Gennaro Tartarisco,³ Maria Di Cicco,¹ Marta Zangani,⁴ Iolanda Chinellato,⁵ Fabrizio Maggi,⁶ Giovanna Tezza,⁵ Pierantonio Macchia,¹ Attilio Boner⁵

► Additional materials are published online only. To view these files please visit the journal online (<http://dx.doi.org/10.1136/thoraxjnl-2011-200137>).

¹Department of Paediatrics, University of Pisa, Pisa, Italy

²Imperial School of Medicine at the National Heart and Lung Institute, London, UK

³Institute of Clinical Physiology, CNR, Pisa, Italy

⁴Department of Diagnostic and Interventional Radiology, University of Pisa, Pisa, Italy

⁵Department of Paediatrics, University of Verona, Verona, Italy

⁶Department of Experimental Pathology, University of Pisa, Pisa, Italy

Correspondence to

Dr Massimo Pifferi, University of Pisa, Department of Pediatrics, Via Roma 67, Pisa 56126, Italy; m.pifferi@med.unipi.it

Received 5 March 2011

Revised 1 June 2012

Accepted 15 June 2012

Published Online First

7 July 2012

ABSTRACT

Background In primary ciliary dyskinesia (PCD) lung damage is usually evaluated by high-resolution CT (HRCT).

Objective To evaluate whether HRCT abnormalities and *Pseudomonas aeruginosa* infection were better predicted by spirometry or plethysmography.

Methods A cross-sectional study performed in consecutive patients with PCD who underwent sputum culture, spirometry, plethysmography and HRCT within 48 h. Principal component analysis and soft computing were used for data evaluation.

Results Fifty patients (26 children) were studied. *P aeruginosa* infection was found in 40% of the patients and bronchiectasis in 88%. There was a correlation between infection with *P aeruginosa* and extent of bronchiectasis ($p=0.009$; $r=0.367$) and air-trapping ($p=0.03$; $r=0.315$). Moreover, there was an association between infection with *P aeruginosa* and residual volume (RV) values $>150\%$ ($p=0.04$) and RV/total lung capacity (TLC) ratio $>140\%$ ($p=0.001$), but not between infection with *P aeruginosa* and forced expiratory volume in 1 s (FEV_1) $<80\%$, or forced expiratory flow between 25% and 75% of forced vital capacity (FVC) ($FEF_{25-75\%}$) $<70\%$ or $FEV_1/FVC <70\%$ ($<80\%$ in children). Severity of the total lung impairment on chest HRCT directly correlated with RV when expressed as per cent predicted ($p=0.003$; $r=0.423$), and RV/TLC ($p<0.001$; $r=0.513$) or when expressed as z scores ($p=0.002$, $r=0.451$ and $p<0.001$, $r=0.536$ respectively). Principal component analysis on plethysmographic but not on spirometry data allowed recognition of different severities of focal air trapping, atelectasis and extent of bronchiectasis.

Conclusions Plethysmography better predicts HRCT abnormalities than spirometry. Whether it might be a useful test to define populations of patients with PCD who should or should not have HRCT scans requires further longitudinal studies.

INTRODUCTION

In primary ciliary dyskinesia (PCD), abnormal motility of respiratory cilia and impaired mucociliary clearance result in recurrent infections of the airways, eventually causing permanent parenchymal damage, and progressive decline in lung function.¹

Chest high-resolution CT (HRCT) has become the method of choice to evaluate structural airway

Key messages

What is the key question?

► Do lung volume measurements predict lung damage better than spirometry in patients with primary ciliary dyskinesia?

What is the bottom line?

► Raised residual volume and residual volume/total lung capacity ratio are associated with *Pseudomonas aeruginosa* infection and with lung damage shown by high-resolution CT.

Why read on?

► The evaluation of static volumes by plethysmography seems to be an underappreciated method for the follow-up of children with primary ciliary dyskinesia; early identification of deterioration in such parameters could result in a more adequate treatment of the disease and in research of eventual unhealthy attitudes of the patients.

changes,² and is used in a number of chronic respiratory diseases including PCD.^{3 4}

However, there is no evidence that regular CT scans affect outcome in PCD⁵ and the potential lifetime cumulative radiation exposure should be considered.^{6 7}

PCD guidelines suggest that lung function should be evaluated at every visit in cooperative children^{1 5 8} since it has been shown that the severity of structural abnormalities may correlate with impairment in forced expiratory volume in 1 s (FEV_1).^{3 4} However, a decreased FEV_1 is not indicative of the site of airway obstruction⁹ and, as in cystic fibrosis,¹⁰ there are preliminary suggestions that PCD is characterised by marked peripheral airway dysfunction.¹¹ Since small airways obstruction may lead to air trapping and to a consequent increase in residual volume (RV) and RV/total lung capacity (TLC) ratio,⁹ we hypothesised that raised functional residual capacity (FRC) made by plethysmography (FRC_{pleth}), and RV and/or RV/TLC ratio, indirect calculated estimates of pulmonary hyperinflation and lung restriction respectively, may be more sensitive than spirometry to structural changes as shown by HRCT in PCD. The aim of the study was to determine the

correlations between HRCT abnormalities and dynamic or static lung function parameters in patients with PCD to assess their potential use as clinical monitoring tools in PCD.¹²

MATERIALS AND METHODS

Subjects

Between March 2008 and May 2010, we enrolled all consecutively newly diagnosed patients with PCD aged ≥ 6 years followed up in the Department of Paediatrics of the University of Pisa. PCD was diagnosed on standard criteria.¹ We obtained sputum, cough swab or pharyngeal aspirate cultures, spirometry, body plethysmography and a HRCT of the chest. A sputum culture was collected, preferably by expectoration. Pharyngeal aspirate was obtained in uncooperative children after an overnight fast using a disposable catheter connected to a mucus extractor inserted into the mouth to a depth of 7–10 cm and drawn back while applying gentle suction.

Informed consent was obtained from adult patients or from the parents of children. The study protocol was approved by the local Hospital Ethical Committee.

Ciliary motion analysis and ultrastructural studies

Samples were obtained from the inferior turbinate using a cytology brush (Microvasive, Milford, Massachusetts, USA) for immediate light microscopy, transmission electron microscopy and cell cultures.¹³ Ciliary morphology, motion pattern, beat frequency, ultrastructural studies and ciliary activity after ciliogenesis in culture were evaluated.^{14–16}

Ciliary motion analysis, ultrastructural assessment and cultures were performed by different operators each one blind to the results obtained by the others.

Lung function

All lung function testing (Master Screen Body equipment; Jaeger, Wuerzburg, Germany) was performed by experienced doctors (MP, MDC) utilising standard American Thoracic Society methodology.^{17, 18} FEV₁, forced vital capacity (FVC), forced expiratory flow between 25% and 75% of FVC (FEF_{25–75%}), FRCpleth, RV, TLC, RV/TLC and parameters of airway mechanics including airway resistance (Raw), specific airway resistance (sRaw) and effective specific resistance (sReff) were expressed as percentage of predicted and z scores values.¹⁹ For plethysmography in each patient we obtained at least three reproducible manoeuvres. To be accepted, single inspiratory manoeuvres needed to have yielded virtually superimposable X–Y plots, and values of FRCpleth had to be within 5% of each other.²⁰

Lung function studies were all performed on the same day, within 2 days of the HRCT.

CT scanning of chest

In all patients chest HRCT was performed using the same scanner (Multislice CT; General Electric Medical Systems, Milwaukee, Michigan, USA). Slices (1 mm thick) were obtained with 10 mm spacing (100–120 kV, 80–130 mA), in the supine position. All images were evaluated by the same radiologist (DC) who was blinded to the clinical data and scored using a modified Bhalla system,²¹ which includes severity of bronchiectasis (score 0–3) and extent of bronchiectasis (score 0–3), mucous plugging (score 0–3), peribronchial thickening (score 0–3), parenchymal abnormalities, such as atelectasis (score 0–3) and focal air-trapping (score 0–3). Bronchiectasis was identified according to standard criteria.²²

Thus, a severity class (from 1 to 3) for total lung impairment was obtained (class of severity 1 for total score of 0–6, class 2 for total score of 7–12, class 3 for total score of 13–18).

Soft computing analysis of data

Data were analysed with soft computing methodologies. Basic elements of soft computing and the application of intelligent control have been recently introduced.²³ The soft computing-based modelling approach was applied to either flow-volume data or body plethysmography or both to develop a model predictive of chest HRCT scores. The model was identified by means of a self-organising artificial neural network (ANN). ANNs are mathematical models in which distributed adaptable parameters are modified through a learning process according to real data. Kohonen self-organising map (KSOM) predictive models were identified to classify chest HRCT scores, (total lung impairment, severity of bronchiectasis, extent of bronchiectasis, peribronchial thickening, mucous plugging, atelectasis, focal air-trapping), starting from flow-volume parameters (FEV₁, FVC, FEV₁/FVC, FEF_{25–75%}), body plethysmography data (FRCpleth, RV, TLC, RV/TLC) and parameters of airway mechanics (Raw, sRaw, sReff). To check the generalisation capability of the neural network, a 10-fold cross-validation process was carried out. In this work, we fixed a 5×5 neurons KSOM with the parameters α (T) = 0.8 and a training of 5000 epochs, which allowed us to obtain the best performance of the model. Further details on KSOM ANNs are reported in the supplementary material online.

Statistical analyses

The principal component analysis (PCA) methodology was applied to display data. PCA is a mathematical linear transformation aimed at reducing the dimensionality of (number of variables in) a dataset to a manageable level while retaining as much as possible of the variance present in the original dataset.²⁴ Data from correlated groups of variables are used to calculate a smaller number of uncorrelated variables (principal components) to simplify further analyses. We used the eigenvalue decomposition²⁴ to obtain the first three principal components in our dataset (denoted Y1, Y2 and Y3) which are associated with 99% of the variance.

There are no data in the published literature to inform a power calculation, so the sample size was opportunistic. Baseline variables were expressed as group mean \pm SD or as median and IQR when the variables were non-normally distributed. Moreover, to allow comparison of observations from different normal distributions, all lung function data were expressed as SD (z) scores.²⁵ Z-score transformation was carried out by using the equation $z = (x - \mu)/\sigma$, where x is the raw score or observation to be standardised, μ is the mean of the reference population, and σ is the SD of the reference population. Differences between means and distributions were evaluated by the two-tailed Student t test.

Correlations between continuous non-normally distributed variables were assessed using Spearman's rank correlation coefficients. One-way analysis of variance (ANOVA) comparing the values of plethysmography indexes between the severity class for total lung impairment at HRCT was also applied. The χ^2 test was used to evaluate the association between *Pseudomonas aeruginosa* (alone or with other bacterial infection) and RV >150%, RV/TLC ratio >140% and FEV₁ <80% or FEF_{25–75%} <70% of predicted. The association between *P. aeruginosa* and FEV₁/FVC <80% predicted for children and <70% predicted for adults was also evaluated. These cut-offs were selected because

Table 1 Spirometry and plethysmography parameters expressed as per cent of predicted and z scores

Functional parameters	% of predicted		z Scores	
	Range	Mean (SD)	Range	Mean (SD)
FEV ₁	31.0–136.0	85.3 (24.6)	–2.82 – 1.47	–0.60 (1.0)
FVC	47.0–138.0	93.4 (18.5)	–2.86 – 2.05	–0.35 (1.0)
FEF _{25/75}	10.0–151.0	63.2 (34.4)	–2.63 – 1.49	–1.07 (1.0)
FEV ₁ /FVC	42.0–98.8	75.45 (13.35)	–2.86 – 1.08	–0.67 (1.0)
Raw	55.4–310.6	164.5 (62.9)	–0.71 – 3.35	1.02 (1.0)
sRaw	71.0–739.2	269.0 (142.0)	–0.20 – 4.50	1.19 (1.0)
sReff	64.0–680.7	240.6 (128.1)	–0.28 – 4.53	1.09 (1.0)
FRC	101.2–248.0	159.3 (31.2)	–0.04 – 4.74	1.90 (1.0)
RV	83.0–397.0	196.5 (69.4)	–0.24 – 4.28	1.39 (1.0)
TLC	85.0–174.0	119.2 (16.7)	–0.89 – 4.46	1.15 (1.0)
RV/TLC	91.0–305.0	161.0 (45.6)	–0.20 – 4.49	1.34 (1.0)

FEV₁, forced expiratory volume in 1 s; FRC, functional residual capacity; FVC, forced vital capacity; Raw, airway resistance; RV, residual volume; sRaw, specific airway resistance; sReff, effective specific resistance; TLC, total lung capacity.

they were previously demonstrated to correlate with air-trapping on HRCT in children.²⁶

A p value <0.05 was considered statistically significant. All statistical calculations were performed using SPSS V.18.0 for Windows (XP/Vista/7).

RESULTS

Fifty patients were studied. Twenty-six were children (19 boys and seven girls, age range 6–17 years, median 11 years; IQR 5.25) and 24 adults (nine men and 15 women, age range 18–47 years, median 30.5 years; IQR 9.5).

Infection with *P. aeruginosa* (with or without other bacteria) was found in 20 (40.0%) patients, seven of whom were children (27% infected). Other organisms (*Serratia marcescens*, *Rhodococcus equi*, *Streptococcus pneumoniae*, *Staphylococcus aureus*, *Enterobacter cloacae*, *Streptococcus pyogenes*, *Alcaligenes xylosoxidans*) were found in 12 (24.0%) subjects.

Results of spirometry and plethysmography expressed as per cent of predicted and as z scores are reported in table 1.

HRCT Bhalla score was 0 in 3 subjects, 1 in 12, 2 in 27, and 3 in the remaining 8 subjects. Bronchiectasis was documented in 44 (88%) patients, 21 of whom were children. Bronchiectasis was present in multiple lobes in 36/44 (82%) subjects. The distribution of bronchiectasis is detailed in table 2.

Patient age was inversely correlated with per cent predicted FEV₁ (p=0.006; r = –0.384), FVC (p=0.04; r = –0.295), FEF_{25–75%} (p=0.01; r = –0.362) and FEV₁/FVC (p=0.02; r = –0.336) but surprisingly not with FRCpleth, RV, TLC and RV/TLC. There was no correlation between patient age and Raw, sRaw or sReff per cent predicted.

Table 2 Bronchiectasis distribution (%) in multiple lobes

Lobes	Right	Left
Upper	20	25
Middle	45	11.4*
Lower	84	70
Lingula	6.8*	16

*In patients with situs inversus.

Considering z scores, patient age was inversely correlated with FEV₁ (p=0.038; r = –0.294), with FEV₁/FVC (p=0.008; r = –0.372) and directly correlated with FVC (p=0.001; r = 0.451), with FRCpleth (p<0.001; r = 0.599), RV (p<0.001; r = 0.623), TLC (p<0.001; r = 0.646) and RV/TLC (p=0.034; r = 0.313). There was no correlation between patient age and Raw, sRaw or sReff z scores.

There was a significant correlation between infection with *P. aeruginosa* and extent of bronchiectasis (p=0.009; r = 0.367) and air-trapping (p=0.03; r = 0.315). Moreover, there was a significant association between infection with *P. aeruginosa* and RV values >150% (p=0.04) and RV/TLC ratio >140% (p=0.001), but not between infection with *P. aeruginosa* and FEV₁<80%, or FEF_{25–75%}<70% or FEV₁/FVC <70% (<80% in children).

There were significant correlations between HRCT scores and lung function parameters. In particular, severity of the total lung impairment on chest HRCT was inversely correlated with FEV₁ (p=0.02; r = –0.322), FVC (p=0.007; r = –0.376), but not with FEF_{25–75%} or FEV₁/FVC, and directly correlated with RV (p=0.003; r = 0.423) (figure 1A) and RV/TLC (p<0.001; r = 0.513) (figure 2A) per cent predicted, but not with TLC. This was confirmed with lung function z scores; severity of the total lung impairment on chest HRCT directly correlated with RV (p=0.002; r = 0.451) (figure 1B), RV/TLC (p<0.001; r = 0.536) (figure 2B) and FRCpleth (p=0.039; r = 0.305), but not with TLC. The correlations between the different HRCT parameters (severity and extent of bronchiectasis, peribronchial thickening, extent of mucous plugging, consolidation or atelectasis and air trapping) and lung function results are reported in tables 3 and 4. As can be seen there were some negative correlations between different HRCT parameters and some per cent predicted spirometry values (table 3) which disappeared when z scores were analysed (table 4). By contrast the positive correlations between severity and extent of bronchiectasis and air trapping with RV and RV/TLC were dependent on whether per cent predicted (table 3) or z scores (table 4) were used.

Moreover, plethysmography indices in patients with different HRCT class severity were found to be significantly different according to one-way ANOVA (p=0.026 for FRCpleth, p=0.007 for RV and p=0.001 for RV/TLC).

Figure 1 (A) Correlation between residual volume per cent predicted (% pred) and total lung impairment severity score at chest high-resolution CT (HRCT). (B) Correlation between residual volume z scores and total lung impairment severity score at chest HRCT.

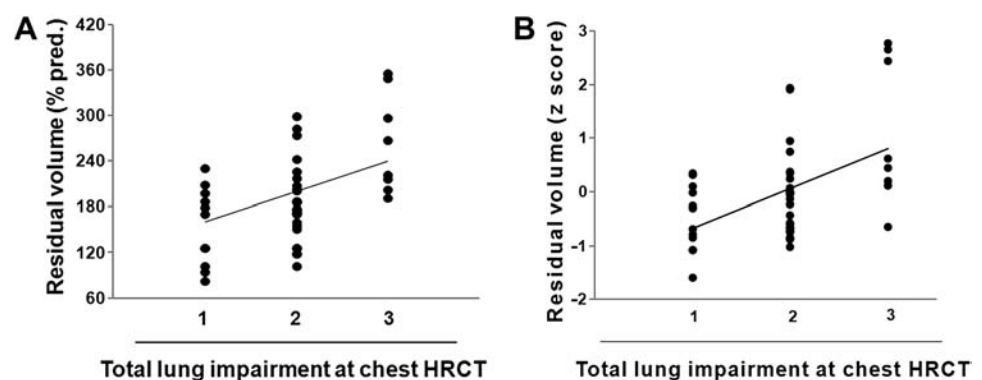
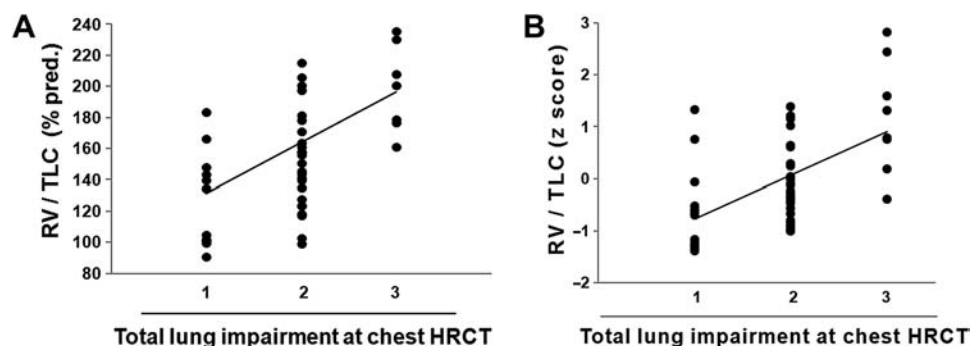


Figure 2 (A) Correlation between residual volume (RV) and total lung capacity (TLC) ratio per cent predicted (% pred) and total lung impairment severity score at chest high-resolution CT (HRCT). (B) Correlation between RV and TLC ratio z scores and total lung impairment severity score at chest HRCT.



Only weak or no correlations were found between the different HRCT parameters and Raw, sRaw and sReff depending on whether per cent predicted values (table 3) or z-scores (table 4) were considered.

Moreover, there was a direct correlation between the age of patients and severity of total lung impairment on chest HRCT ($p=0.002$; $r=0.425$), and severity ($p=0.004$; $r=0.404$) and extent of bronchiectasis ($p<0.001$; $r=0.510$), but not with focal air-trapping scores or other parameters.

PCA performed using the body plethysmography data is depicted in figure 3, which shows three-dimensional scatter plots of the first four principal components evaluated processing the original body plethysmography variables (FRCpleth, RV, TLC and RV/TLC ratio), after the removal of an outlier. Each scatter plot shows the differences between scores 1 and 3 for focal air-trapping (figure 3A), atelectasis (figure 3B), extent of bronchiectasis (figure 3C) and total lung impairment (figure 3D). The PCA topological study allows focal air-trapping severity, atelectasis and the extent of bronchiectasis to be visually discriminated, although the clusters overlap. The analysis does not allow severity of bronchiectasis, peribronchial thickening and mucous plugging to be discriminated. The PCA topological study of flow–volume data and of airway mechanics parameters (Raw, sRaw and sReff) does not permit any discrimination of chest HRCT scores. The PCA topological study does not identify patients with *P aeruginosa* infection. Further results obtained by KSOM models are reported in the supplementary material online.

DISCUSSION

Statement of principal findings

To our knowledge this is the largest dataset of contemporaneous spirometry, plethysmography and HRCT in patients with PCD. HRCT was performed in all patients aged 6 years or older because it is known that from this age many patients already

have some degree of bronchiectasis²⁷ and from this age patients can both cooperate with the procedure and be able to perform reproducible lung function testing.²⁸

We show that soft computing based on plethysmographic lung volumes, but not spirometry, is sensitive to a range of HRCT abnormalities. Reduction in lung function associated with bronchiectasis has been previously reported in patients with PCD.^{12–29} However, we report for the first time that FRCpleth, RV and RV/TLC ratio is associated with the severity of air trapping, atelectasis and extent of bronchiectasis and with *P aeruginosa* infection. Hence follow-up of PCD patients may be preferable with plethysmography rather than simple spirometry.

Strengths and weaknesses of the study

Our study has some strengths. First the completeness of ascertainment, since all patients performed all the tests, obviating selection bias. Second all the evaluations were done within 48 h. Third the objective analytical techniques using soft computing greatly reduces the chance of investigator bias.

Strengths and weaknesses in relation to other studies

In our study group the vast majority of adults and 80% of the children had bronchiectasis and, as previously reported, half of the adults²⁹ and approximately one-third of the children had chronic *Paeruginosa* infection. The latter was associated with air-trapping, as previously documented in young children with cystic fibrosis.³⁰ Focal air-trapping, which indicates small airways disease, probably starts early and our results document that static lung volume evaluation can detect this even in younger patients. This finding lends further support to the hypothesis that peripheral lung damage may be an early event in PCD.¹⁰

It has recently been suggested that even the youngest patients already have irreversible lung damage¹² and that bronchiectasis,

Table 3 Correlation between chest high-resolution CT and functional parameters expressed as per cent of predicted normal

HRCT parameters	FEV ₁	FVC	FEF _{25–75%}	FEV ₁ /FVC	Raw	sRaw	sReff	FRCpleth	RV	TLC	RV/TLC
Severity of bronchiectasis	$p=0.01$ $r=-0.350$	$p=0.005$ $r=-0.393$	NS	NS	NS	NS	NS	NS	$p=0.02$ $r=0.331$	NS	$p=0.005$ $r=0.408$
Extent of bronchiectasis	$p=0.01$ $r=-0.346$	$p=0.01$ $r=-0.356$	$p=0.02$ $r=-0.316$	NS	NS	NS	NS	NS	$p=0.02$ $r=0.336$	NS	$p=0.001$ $r=0.459$
Peribronchial thickening	NS	NS	NS	NS	NS	NS	NS	NS	NS	NS	NS
Extent of mucous plugging	NS	NS	NS	NS	$p=0.035$ $r=0.315$	$p=0.044$ $r=0.301$	NS	NS	NS	NS	NS
Consolidation or atelectasis	NS	NS	NS	NS	NS	NS	NS	NS	NS	NS	NS
Air-trapping	$p=0.01$ $r=-0.341$	NS	$p=0.01$ $r=-0.362$	$p=0.04$ $r=-0.291$	NS	$p=0.027$ $r=0.327$	$p=0.023$ $r=0.334$	$p=0.002$ $r=0.438$	$p<0.001$ $r=0.728$	$p=0.008$ $r=0.389$	$p<0.001$ $r=0.757$

FEF_{25–75%}, forced expiratory flow between 25% and 75% of forced vital capacity; FEV₁, forced expiratory volume in 1 s; FRCpleth, functional residual capacity by plethysmography; FVC, forced vital capacity; HRCT, high-resolution CT; NS, non-significant; Raw, airway resistance; RV, residual volume; sRaw, specific airway resistance; sReff, effective specific resistance; TLC, total lung capacity.

Table 4 Correlations between chest high-resolution CT and functional parameters expressed as z scores

HRCT parameters	FEV ₁	FVC	FEF _{25–75%}	FEV ₁ /FVC	Raw	sRaw	sReff	FRCpleth	RV	TLC	RV/TLC
Severity of bronchiectasis	NS	NS	NS	NS	NS	p=0.034 r=0.313	p=0.049 r=0.293	p=0.027 r=0.326	p=0.002 r=0.445	p=0.050 r=0.291	p=0.004 r=0.421
Extent of bronchiectasis	NS	NS	NS	NS	NS	p=0.019 r=0.344	p=0.025 r=0.331	p=0.002 r=0.446	p<0.001 r=0.547	p=0.039 r=0.306	p<0.001 r=0.519
Peribronchial thickening	NS	NS	NS	NS	NS	NS	NS	NS	NS	NS	NS
Extent of mucous plugging	NS	NS	NS	NS	p=0.049 r=0.295	NS	NS	NS	NS	NS	NS
Consolidation or atelectasis	NS	NS	NS	NS	NS	NS	NS	NS	NS	NS	NS
Air-trapping	NS	NS	NS	NS	NS	NS	NS	p=0.012 r=0.367	p=0.001 r=0.483	NS	p<0.001 r=0.696

FEF_{25–75%}, forced expiratory flow between 25% and 75% of forced vital capacity; FEV₁, forced expiratory volume in 1 s; FRCpleth, functional residual capacity by plethysmography; FVC, forced vital capacity; HRCT, high-resolution CT; NS, non-significant; Raw, airway resistance; RV, residual volume; sRaw, specific airway resistance; sReff, effective specific resistance; TLC, total lung capacity.

reduction in lung flows and increased RV and RV/TLC can be present in patients with PCD as young as <3 years.³¹ We were not able to determine this because we could not study very young children with PCD.

Meaning of the study

Our findings suggest that lung disease in PCD begins early and that it is better identified at least in school-aged children and adults by the finding of air-trapping or HRCT, rather than

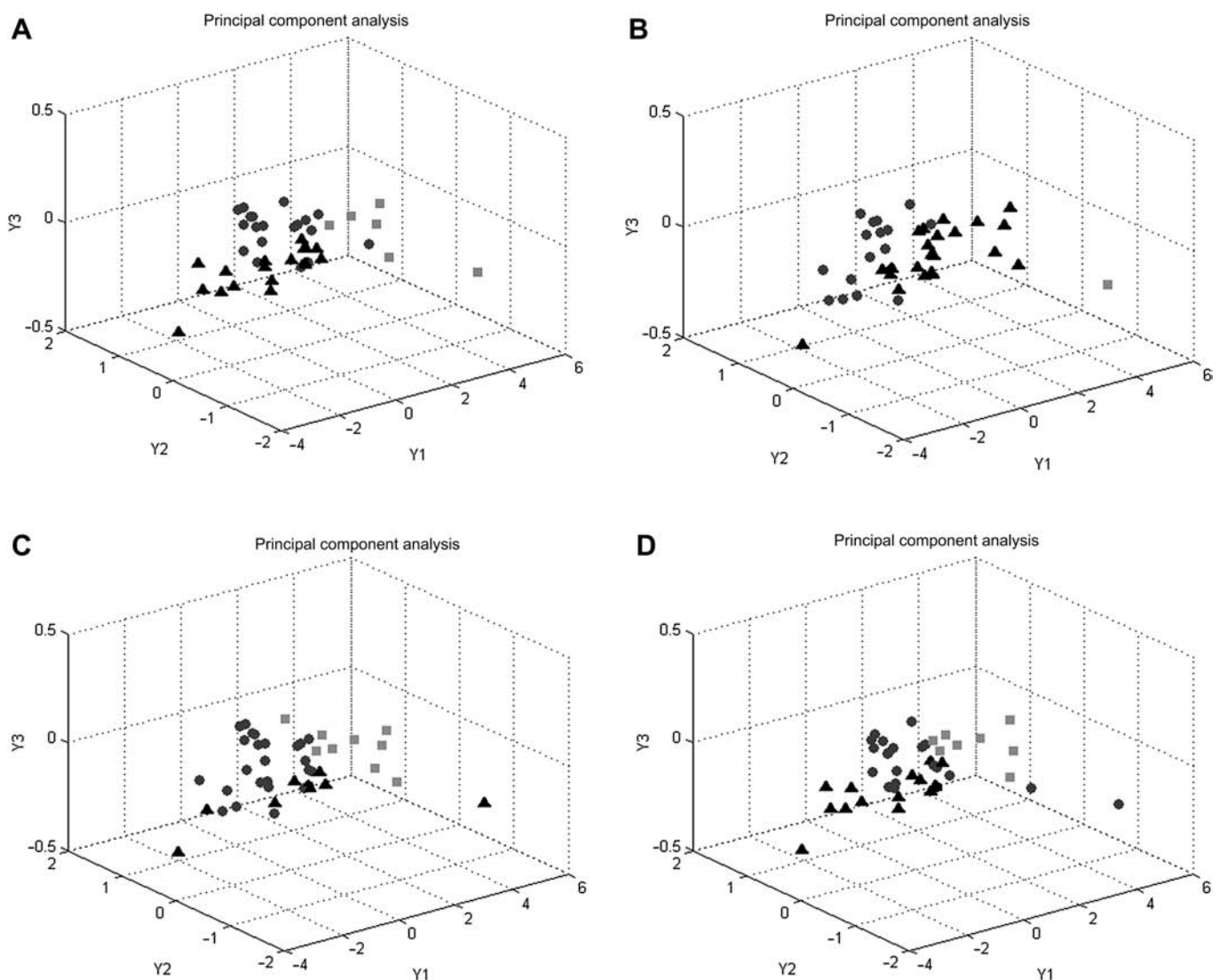


Figure 3 (A) Three-dimensional scatter plots for air-trapping score 1 (triangles), 2 (circles), 3 (squares) in relation to functional residual capacity by plethysmography (FRCpleth), residual volume (RV), total lung capacity (TLC) and RV/TLC ratio. (B) Three-dimensional scatter plots for atelectasis score 1 (triangles), 2 (circles), 3 (squares) in relation to FRCpleth, RV, TLC and RV/TLC ratio. (C) Three-dimensional scatter plots for bronchiectasis extension score 1 (triangles), 2 (circles), 3 (squares) in relation to FRCpleth, RV, TLC and RV/TLC ratio. (D) Three-dimensional scatter plots for total lung impairment score 1 (triangles), 2 (circles), 3 (squares) in relation to FRCpleth, RV, TLC and RV/TLC ratio.

spirometry. In previous studies of adults and children with PCD, total lung abnormalities and bronchiectasis severity on HRCT were shown to be related to FEV₁ and FVC.^{3,4} Our results do not confirm this in a larger series of PCD, even when analysed using a soft computing-based modelling approach, but instead suggest that plethysmography is a much more sensitive test.

CT scanning of the chest has become a popular tool to monitor patients with cystic fibrosis,³² a disease that has similarities with PCD. However, no study has evaluated the impact of such monitoring on health outcomes or on clinical decision-making in patients with PCD or cystic fibrosis. Moreover, there are concerns on the uncritical use of high-tech medical imaging and on the potential harm of repeated radiological exposures, particularly in children with lifelong diseases.^{6,7} Consequently, careful thought is needed before requesting repeated chest CT scans. By contrast a detailed evaluation of lung volumes is only limited by the availability of the equipment, and by the ability of the technician to obtain patients' collaboration, but this is usually not a problem in the specialist centres that should care for these patients.

Unanswered questions and future research

Even though we have not studied very young subjects, from our results it is tempting to speculate that accumulation of secretions, in the early stages of disease, may induce primarily an obstruction in terminal bronchioles which may go undetected for a long period during alveolar growth of the lung. The consequent focal air-trapping during this phase of alveolar growth might lead to impaired septation and decreased elastic recoil as has been observed in animal models.³³ Early structural changes in the distal airways could explain why we found a lack of correlation between per cent predicted RV and RV/TLC with age, unlike for spirometry, which may reflect slower progressive, age-related damage to large airways. To confirm this hypothesis, data are required from a longitudinal study in patients with PCD from the newborn period, using age-appropriate physiological techniques.

Although our findings show the superior sensitivity of plethysmography over spirometry in detecting HRCT changes in PCD, the findings need to be validated in a second cohort of patients. It would be valuable to compare plethysmography with sophisticated assessments of distal airway function, such as lung clearance index³⁴ and distal airway production of exhaled nitric oxide in PCD.^{35–37}

Longitudinal data are needed to determine which technique is more sensitive to a change in the patient's condition. Finally, comparisons of plethysmography and spirometry in other airway diseases and in longitudinal studies would be of interest.

In conclusion, in this group who have a high pretest probability of lung damage,²⁷ and given the different correlations between the various lung function parameters and HRCT-derived lung disease scores we suggest that measurement of lung volumes rather than spirometry may be preferable in the routine clinical management of PCD. Furthermore, this may reduce the number of scans used to monitor disease progression, although this needs testing prospectively. As with all investigations, HRCT should be requested only when the results are going to change the therapeutic strategy in the individual patient, or as part of an ethically approved, focused-research protocol.⁸ Our data represent training results and further work would be required to establish predictive validity, in particular in a second cohort studied longitudinally.

Acknowledgements We wish to thank the Editor and the reviewers for their help in the evaluation of our data.

Contributors M Pifferi: contributed to study design, data evaluation and drafting and revising the submitted manuscript. He had full access to all of the data in the study and he takes full responsibility for the integrity of all of the data and the accuracy of the data analysis. A Bush: contributed to data evaluation and drafting and revising the submitted manuscript. G Pioggia: contributed to data analysis and drafting the submitted manuscript. D Caramella: contributed to data analysis and drafting the submitted manuscript. G Tartarisco: contributed to data analysis and drafting the submitted manuscript. M Di Cicco: contributed to collecting data. M Zangani: contributed to collecting data. I Chinellato: contributed to collecting data. F Maggi performed the statistical analysis. G Tezza: contributed to the reevaluation of all data after reviewers' comments. P Macchia: contributed to study design. A L Boner: contributed to study design, data evaluation and drafting and revising the submitted manuscript.

Funding This research was supported by the Fondazione Carlo Laviosa, Italy.

Competing interests None declared.

Patient consent Obtained.

Ethics approval Ethics approval was provided by Hospital Ethical Committee of Pisa.

Provenance and peer review Not commissioned; externally peer reviewed.

REFERENCES

1. Bush A, Chodhari R, Collins N, *et al*. Primary ciliary dyskinesia: current state of the art. *Arch Dis Child* 2007;**92**:1136–40.
2. Rossi UG, Owens CM. The radiology of chronic lung disease in children. *Arch Dis Child* 2005;**90**:601–7.
3. Kennedy MP, Noone PG, Leigh MW, *et al*. High-resolution CT of patients with primary ciliary dyskinesia. *AJR Am J Roentgenol* 2007;**188**:1232–8.
4. Santamaria F, Montella S, Tiddens HA, *et al*. Structural and functional lung disease in primary ciliary dyskinesia. *Chest* 2008;**134**:351–7.
5. Barbato A, Frischer T, Kuehni CE, *et al*. Primary ciliary dyskinesia: a consensus statement on diagnostic and treatment approaches in children. *Eur Respir J* 2009;**34**:1264–76.
6. Brody AS, Frush DP, Huda W, *et al*. Radiation risk to children from computed tomography. *Pediatrics* 2007;**120**:677–82.
7. Brenner DJ, Hall EJ. Computed tomography—an increasing source of radiation exposure. *N Engl J Med* 2007;**357**:2277–84.
8. Fauroux B, Tamalet A, Clément A. Management of primary ciliary dyskinesia: the lower airways. *Paediatr Respir Rev* 2009;**10**:55–7.
9. Stănescu D. Small airways obstruction syndrome. *Chest* 1999;**116**:231–3.
10. Tiddens HA, Donaldson SH, Rosenfeld M, *et al*. Cystic fibrosis lung disease starts in the small airways: can we treat it more effectively? *Pediatr Pulmonol* 2010;**45**:107–17.
11. Green K, Buchvald FF, Marthin JK, *et al*. Ventilation inhomogeneity in children with primary ciliary dyskinesia. *Thorax* 2012;**67**:49–53.
12. Marthin JK, Petersen N, Skovgaard LT, *et al*. Lung function in patients with primary ciliary dyskinesia: a cross-sectional and 3-decade longitudinal study. *Am J Respir Crit Care Med* 2010;**181**:1262–8.
13. Rutland J, Cole PJ. Non-invasive sampling of nasal cilia for measurement of beat frequency and study of ultrastructure. *Lancet* 1980;**2**:564–5.
14. Pifferi M, Cangiotti AM, Ragazzo V, *et al*. Primary ciliary dyskinesia: diagnosis in children with inconclusive ultrastructural evaluation. *Pediatr Allergy Immunol* 2001;**12**:274–82.
15. Carlén B, Stenram U. Ultrastructural diagnosis in the immotile cilia syndrome. *Ultrastruct Pathol* 1987;**11**:653–8.
16. Pifferi M, Montemurro F, Cangiotti AM, *et al*. Simplified cell culture method for the diagnosis of atypical primary ciliary dyskinesia. *Thorax* 2009;**64**:1077–81.
17. American Thoracic Society. Standardization of spirometry: 1994 update. *Am J Respir Crit Care Med* 1995;**152**:1107–36.
18. American Association for Respiratory Care. Clinical Practice Guideline: static lung volumes: 2001 revision & update. *Respir Care* 2001;**46**:531–9.
19. Zapletal A, Samánek M, Paul T. *Lung Function in Children and Adolescents: Methods, Reference Values*. Basel, Switzerland: S Karger AG, 1987.
20. Coates AL, Peslin R, Rodenstein D, *et al*. Measurement of lung volumes by plethysmography. *Eur Respir J* 1997;**10**:1415–27.
21. Bhalla M, Turcios N, Aponte V, *et al*. Cystic fibrosis: scoring system with thin-section CT. *Radiology* 1991;**179**:783–8.
22. Pifferi M, Caramella D, Bulleri A, *et al*. Pediatric bronchiectasis: correlation of HRCT, ventilation and perfusion scintigraphy, and pulmonary function testing. *Pediatr Pulmonol* 2004;**38**:298–303.
23. Jamshidi M. Tools for intelligent control: fuzzy controllers, neural networks and genetic algorithms. *Philos Transact A Math Phys Eng Sci* 2003;**361**:1781–808.
24. Shaw PJ. *Multivariate Statistics for the Environmental Sciences*. London, UK: Hodder Arnold, 2003.
25. Dibley MJ, Goldsby JB, Staehling NW, *et al*. Development of normalized curves for the international growth reference: historical and technical considerations. *Am J Clin Nutr* 1987;**46**:736–48.

26. **Pifferi M**, Caramella D, Ragazzo V, *et al*. Low-density areas on high-resolution computed tomograms in chronic pediatric asthma. *J Pediatr* 2002;**141**:104–8.
27. **Jain K**, Padley SP, Goldstraw EJ, *et al*. Primary ciliary dyskinesia in the paediatric population: range and severity of radiological findings in a cohort of patients receiving tertiary care. *Clin Radiol* 2007;**62**:986–93.
28. **Davis SD**, Brody AS, Emond MJ, *et al*. Endpoints for clinical trials in young children with cystic fibrosis. *Proc Am Thorac Soc* 2007;**4**:418–30.
29. **Noone PG**, Leigh MW, Sannuti A, *et al*. Primary ciliary dyskinesia: diagnostic and phenotypic features. *Am J Respir Crit Care Med* 2004;**169**:459–67.
30. **Dakin CJ**, Numa AH, Wang H, *et al*. Inflammation, infection, and pulmonary function in infants and young children with cystic fibrosis. *Am J Respir Crit Care Med* 2002;**165**:904–10.
31. **Brown DE**, Pittman JE, Leigh MW, *et al*. Early lung disease in young children with primary ciliary dyskinesia. *Pediatr Pulmonol* 2008;**43**:514–16.
32. **Robinson TE**. Computed tomography scanning techniques for the evaluation of cystic fibrosis lung disease. *Proc Am Thorac Soc* 2007;**4**:310–15.
33. **Srinivasan G**, Bruce EN, Houtz PK, *et al*. Dexamethasone-induced changes in lung function are not prevented by concomitant treatment with retinoic acid. *Am J Physiol Lung Cell Mol Physiol* 2002;**283**:L275–87.
34. **Gustafsson PM**, De Jong PA, Tiddens HA, *et al*. Multiple-breath inert gas washout and spirometry versus structural lung disease in cystic fibrosis. *Thorax* 2008;**63**:129–34.
35. **Corbelli R**, Bringolf-Isler B, Amacher A, *et al*. Nasal nitric oxide measurements to screen children for primary ciliary dyskinesia. *Chest* 2004;**126**:1054–9.
36. **Mateos-Corral D**, Coombs R, Grasemann H, *et al*. Diagnostic value of nasal nitric oxide measured with non-velum closure techniques for children with primary ciliary dyskinesia. *J Pediatr* 2011;**159**:420–4.
37. **Pifferi M**, Bush A, Maggi F, *et al*. Nasal nitric oxide and nitric oxide synthase expression in primary ciliary dyskinesia. *Eur Respir J* 2011;**37**:572–7.

student
BMJ



Join the
BMA and receive
Student BMJ for free.
Visit: [bma.org.uk/
membership](http://bma.org.uk/membership)

What medical students need to know
but won't find in a textbook

Don't miss out. Subscribe for just £48 a year*

student.bmj.com

*Price excludes tax, valid for personal subscriptions only

KOHONEN MAP FOCAL AIR TRAPPING

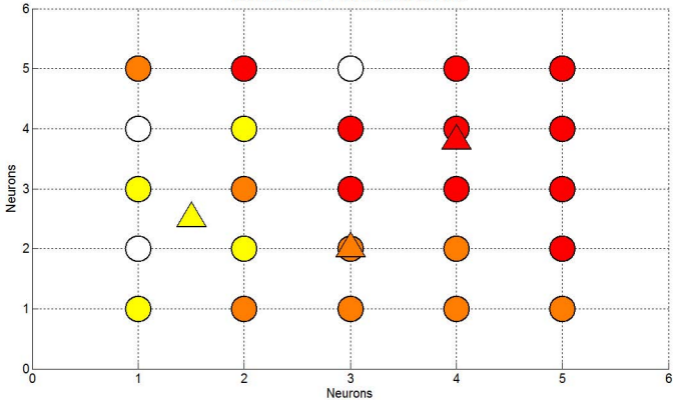


Fig. 4a

KOHONEN MAP ATELECTASIS

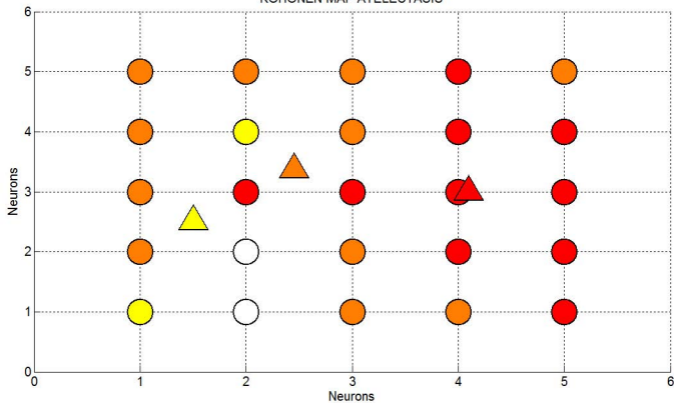


Fig. 4b

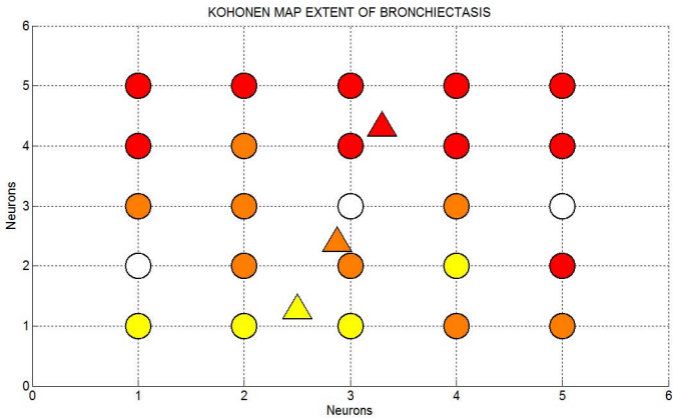


Fig. 4c

KOHONEN MAP TOTAL LUNG

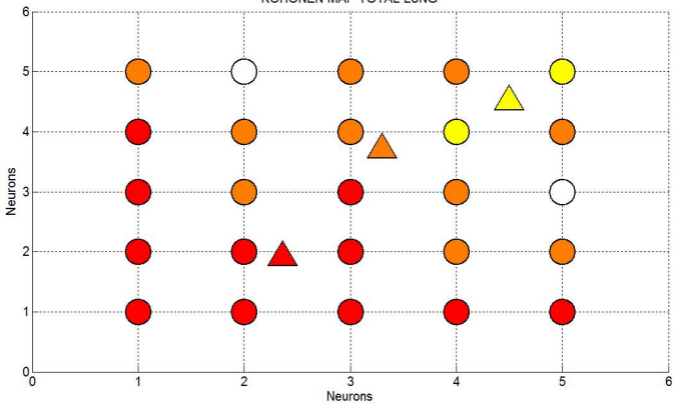


Fig. 4d

EVALUATION OF PULMONARY DISEASE USING STATIC LUNG VOLUMES MEASUREMENT IN PRIMARY CILIARY DYSKINESIA

ONLINE DATA REPOSITORY

Soft computing analysis of data

The Principal Component Analysis (PCA) methodology was applied to display data. PCA is a mathematical linear transformation aimed to scale the data in a three-dimensional uncorrelated space, in order to display statistically meaningful differences among the original variables while retaining as much as possible of the variance present in the original dataset. PCA projects the original data along new uncorrelated variables called principal components, i.e. the directions where the variances of data are maximized. These directions are determined by the eigenvectors of the covariance matrix of the original data corresponding to the largest eigenvalues. The prefix eigen- is adopted from the German word "eigen" for "own" in the sense of a characteristic description. The magnitude of the eigenvalues corresponds to the variance of the data along the eigenvector directions. In fact, for a given p -dimensional data set X , the m principal components Y_1, Y_2, \dots, Y_m , where $1 < m < p$, are orthonormal axes evaluated by the m leading eigenvectors of the covariance matrix, onto which the retained variance is maximum. The information of the observation vectors is contained in the subspace spanned by the first m principal components. Therefore, each original data vector can be represented by its principal component vector with dimensionality.

Data were analyzed with soft computing methodologies. Basic elements of soft computing and the application of intelligent control have been recently introduced. The term soft computing denotes methodologies that seek to integrate arithmetical computing, reasoning and decision making into a framework trading off precision and uncertainty. The methodologies used are fuzzy logic, neural networks (NNs) and genetic algorithms and programming. [1] Soft computing-based models are capable of analyzing complex medical data, exploiting meaningful relationships in a data set to help physicians in the diagnosis, treatment and recognition of the clinical outcomes.

KSOMs are artificial neural networks in which the learning process is unsupervised, i.e. the distributed adaptable parameters of the model are autonomously organized on the data. The learning process produces a two-dimensional discrete representation, i.e. a map, of the input space of the input data. Self-organizing maps are different from other artificial neural networks in the sense that they use a neighborhood function to preserve the topological properties of the input space. This makes self-organizing maps useful for visualizing low-dimensional views of high-dimensional data, akin to multidimensional scaling. Such models were first described as artificial neural networks by the Professor Teuvo Kohonen (2).

KSOM is a two-dimensional ANN-based model able to solve classification tasks exploiting structures in the data through an unsupervised learning process.(3) A KSOM maps the original space into a two-dimensional net of neurons in such a way that close neurons respond to similar signals, in order to solve classification tasks and to find structures in data. KSOMs are unsupervised neural networks, i.e. they exploit similarities of samples apart from the class which they belong. In the unsupervised training process, the synaptic weight vectors of the artificial neurons of the KSOM are adapted by means of the training data set examples in such a way that the KSOM supplies as good a representation as possible of the training data set.

The KSOM is composed by an input layer and an output layer . Let X represents the input vector, W the matrix of weights, and Y the output neurons. During the training of the model, at time t , for each output neuron j , the activation is evaluated by the Euclidean distance, i.e. $Y_j = \| W_j(t) - X(t) \|$. The neuron with the minimum activation is the winning neuron. The weight w_{ij} of a generic neuron i at the time T , for the input vector f is modified as follows: $w_{ij}(T) = w_{ij}(T-1) + \alpha(T)[f(T) - w_{ij}(T-1)]$ where $\alpha(T)$ is the gain coefficient selected in the range $(0,1)$. The response of the KSOM is a boolean vector; each element represents the activation function of a neuron. After the training process, a supervised labelling step is performed. Cluster labels are assigned to the individual artificial neurons. After validation of the KSOM by the data set, performance of the classification task is commonly evaluated using the confusion matrix. In order to check the generalization

capability of the neural network, a 10-fold cross-validation process is carried out. In this work, we fixed a 5x5 neurons KSOM with the parameters $\alpha(T) = 0.8$ and a training of 5000 epochs, which allows to obtain the best performance of the model.

The performances of a KSOM predicting model are assessed by using the confusion matrix, which the generic elements i, j indicate how many times in mean percentage \pm SD a pattern belonging to the class i was classified as belonging to the class j . In order to check the generalization capability of the KSOM, a k -fold cross-validation is carried out; each fold consists of randomly selected samples, at least one for each category index was included in each fold.

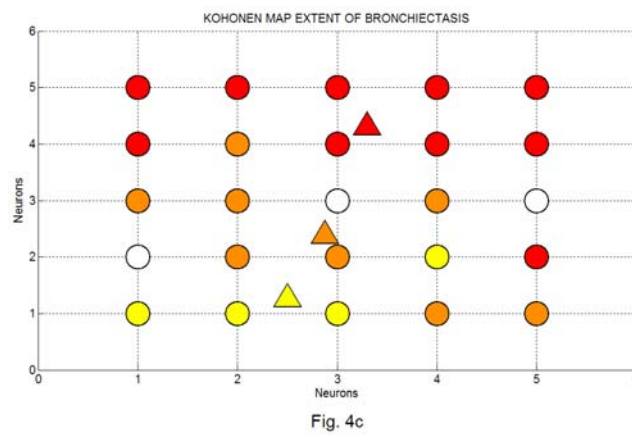
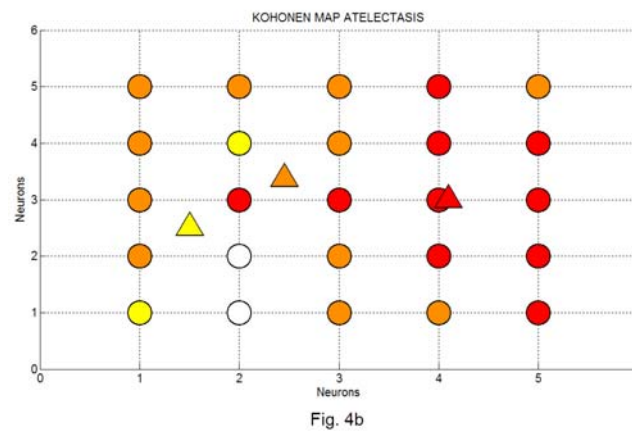
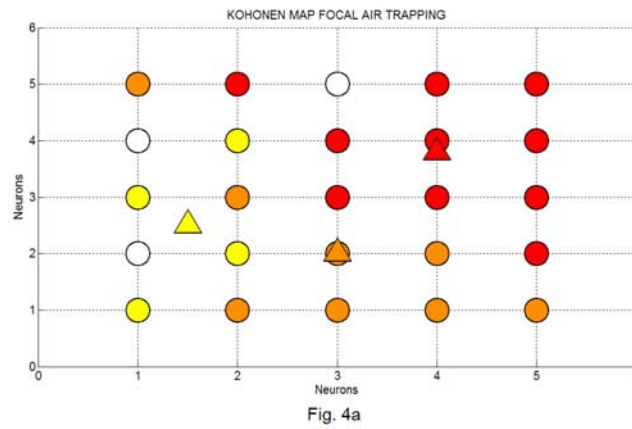
RESULTS

In order to explore the discriminatory power of spirometry and body plethysmography variables in terms of chest HRCT scores and chronic infection with *Pseudomonas aeruginosa* infection, two KSOM models were identified. A ten-fold cross-validation procedure was applied in order to test the performance of each KSOM model.

The identified model based on FEV₁ alone or in combination with FVC, FEV₁/FVC and FEF₂₅₋₇₅, is not able to identify any chest HRCT score. The identified model based on body plethysmography variables, alone or in combination, is able to discriminate focal air-trapping severity, atelectasis and the extent of bronchiectasis HRCT scores. The mean \pm SD percentages of the confusion matrices obtained by the analysis of the focal air-trapping severity, the atelectasis and the extension of bronchiectasis are reported in table 1. In particular, the KSOM model correctly identifies focal air-trapping with percentages of correct classifications of 94.5%, 77.3 and 81.0% for class of severity 1, 2 and 3 respectively, using the body plethysmography data; whilst using spirometry the discriminatory power is very low (42.0%, 32.5% and 35.0%). The visual representation of the KSOM model based on body plethysmography for the focal air-trapping classification is shown in Figure 4a. Likewise, the model correctly identifies atelectasis and the extent of bronchiectasis with percentages of correct classifications of 66%, 60% and 78.0%, and 79.%, 59.% and of 80.0%, respectively, using the body plethysmography data; by contrast, using spirometry the discriminatory

power is very low (40.0%, 25.0 and 38.6%, and 23.0%, 28.33% and 55.0%). The visual representations of the KSOM models respectively for the atelectasis and the extent of bronchiectasis classifications based on body plethysmography are shown in Figures 4b and 4c respectively. The model correctly identifies the total score with percentages of correct classifications of 80.3%, 63.3% and 90% using the body plethysmography data; while using spirometry does not allow any discrimination (30.0%, 23.3 and 55.0%). The visual representation of the KSOM model based on body plethysmography for the total score classification is shown in Figure 4d. With regard to the other HRCT variables (severity of bronchiectasis, peribronchial thickening and mucous plugging), the model shows the same low discriminatory power as spirometry. These results demonstrate the high discriminatory power of the body plethysmography as compared to spirometry. The identified model based on spirometry and body plethysmography data, alone or in combination, is not able to identify those chronically infected with *Pseudomonas*.

1. Zadeh LA. The evolution of systems analysis and control: a personal perspective. IEEE Control Syst 1996;16: 95–8.
2. Kohonen T. Honkela, T. Kohonen network. Scholarpedia; 2007;2:1568.
http://www.scholarpedia.org/article/Kohonen_network. (accessed 10 October 2010)
3. Honkela, T. Self-Organizing Maps in Natural Language Processing. Thesis for the degree of Doctor of Philosophy Espoo, Finland 1997. <http://users.ics.tkk.fi/tho/thesis/> (accessed 12 October 2010).



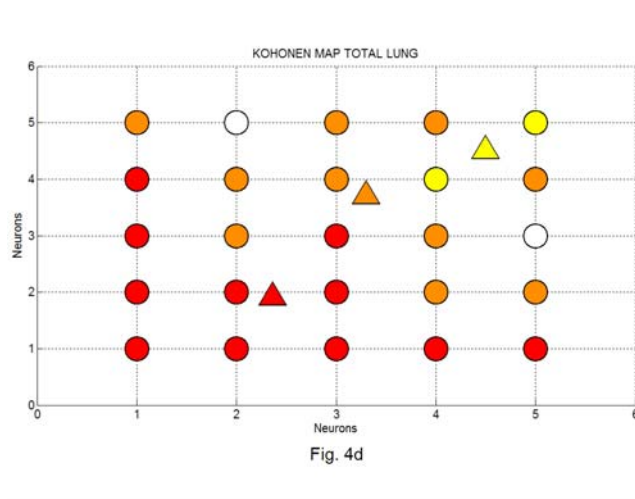


Figure 4 – Visual representations of the KSOMs based on body plethysmography - red: class of severity 1; orange: class of severity 2; yellow: class of severity 3; each triangle indicates the centroid of the corresponding cluster; the inactivated neurons are reported in white; a) focal air-trapping; b) atelectasis; c) the extension of bronchiectasis; d) total score.

**EVALUATION OF PULMONARY DISEASE USING STATIC LUNG VOLUMES
MEASUREMENT IN PRIMARY CILIARY DYSKINESIA
ONLINE DATA REPOSITORY**

<i>Focal Air Trapping</i>									
	<i>Plethysmography</i>			<i>Spirometry</i>			<i>Raw, sRaw and sReff</i>		
	<i>Score 1</i>	<i>Score 2</i>	<i>Score 3</i>	<i>Score 1</i>	<i>Score 2</i>	<i>Score 3</i>	<i>Score 1</i>	<i>Score 2</i>	<i>Score 3</i>
<i>Score 1</i>	93.2 ± 0.1	5 ± 0.18	1.8 ± 0.12	42 ± 0.19	28 ± 0.19	30 ± 0.17	50 ± 0.15	34.33 ± 0.23	15.67 ± 0.2
<i>Score 2</i>	9.8 ± 0.12	78.6 ± 0.16	11.6 ± 0.7	37.5 ± 0.24	32.5 ± 0.17	30 ± 0.19	51.66 ± 0.31	37.5 ± 0.13	10.9 ± 0.17
<i>Score 3</i>	11.9 ± 0.24	8.1 ± 0.11	80 ± 0.22	15 ± 0.24	50 ± 0.23	35 ± 0.24	35 ± 0.32	35 ± 0.13	30 ± 0.33
<i>Atelectasis</i>									
	<i>Plethysmography</i>			<i>Spirometry</i>			<i>Raw, sRaw and sReff</i>		
	<i>Score 1</i>	<i>Score 2</i>	<i>Score 3</i>	<i>Score 1</i>	<i>Score 2</i>	<i>Score 3</i>	<i>Score 1</i>	<i>Score 2</i>	<i>Score 3</i>
<i>Score-1</i>	65.2 ± 0.21	13.1 ± 0.15	21.7 ± 0.19	40 ± 0.37	15 ± 0.21	45 ± 0.37	10 ± 0.11	73.33 ± 0.23	16.6 ± 0.34
<i>Score 2</i>	28.1 ± 0.3	61.3 ± 0.2	10.6 ± 1.1	52 ± 0.21	25 ± 0.37	23 ± 0.11	31.66 ± 0.14	23.33 ± 0.19	45.0 ± 0.12
<i>Score 3</i>	10.3 ± 0.25	12.6 ± 0.08	77.1 ± 0.2	41.4 ± 0.18	20 ± 0.12	38.6 ± 0.12	34 ± 0.24	21 ± 0.21	45 ± 0.26
<i>Extension of Bronchiectasis</i>									
	<i>Plethysmography</i>			<i>Spirometry</i>			<i>Raw, sRaw and sReff</i>		
	<i>Score 1</i>	<i>Score 2</i>	<i>Score 3</i>	<i>Score 1</i>	<i>Score 2</i>	<i>Score 3</i>	<i>Score 1</i>	<i>Score 2</i>	<i>Score 3</i>
<i>Score 1</i>	80.3 ± 0.18	16.1 ± 0.5	3.6 ± 0.18	23 ± 0.33	63.33 ± 0.29	13 ± 0.23	30 ± 0.24	65 ± 0.32	5 ± 0.15
<i>Score 2</i>	20.6 ± 0.6	58.4 ± 0.8	21 ± 0.21	41.66 ± 0.26	28.33 ± 0.13	30.00 ± 0.17	25 ± 0.12	60 ± 0.15	15 ± 0.66
<i>Score 3</i>	11.8 ± 0.11	12 ± 0.14	76.2 ± 0.26	20 ± 0.25	25 ± 0.35	55 ± 0.28	15 ± 0.23	55 ± 0.41	30 ± 0.4
<i>Total Score</i>									
	<i>Plethysmography</i>			<i>Spirometry</i>			<i>Raw, sRaw and sReff</i>		
	<i>Score 1</i>	<i>Score 2</i>	<i>Score 3</i>	<i>Score 1</i>	<i>Score 2</i>	<i>Score 3</i>	<i>Score 1</i>	<i>Score 2</i>	<i>Score 3</i>
<i>Score 1</i>	79.3 ± 0.19	14.1 ± 0.23	6.6 ± 0.15	30 ± 0.18	63.33 ± 0.19	6.6 ± 0.14	41 ± 0.27	43 ± 0.24	16 ± 0.19
<i>Score 2</i>	18.7 ± 0.11	61.3 ± 0.17	20 ± 0.13	41.66 ± 0.18	23.33 ± 0.11	35.0 ± 0.16	29.5 ± 0.31	45.5 ± 0.32	25 ± 0.21
<i>Score 3</i>	5.4 ± 0.15	5 ± 0.23	89.6 ± 0.27	15 ± 0.24	10 ± 0.21	55 ± 0.26	24 ± 0.33	40 ± 0.43	36 ± 0.34

Table 1. Models based on body plethysmography, spirometry, or parameters of airway mechanics (Raw, sRaw and sReff) (expressed as % pred.) and correct recognition (expressed as mean ± standard deviation) of focal air-trapping and atelectasis severity, extension of bronchiectasis, and total lung impairment on chest HRCT, respectively.

**EVALUATION OF PULMONARY DISEASE USING STATIC LUNG VOLUMES
MEASUREMENT IN PRIMARY CILIARY DYSKINESIA
ONLINE DATA REPOSITORY**

<i>Focal Air Trapping</i>									
	<i>zRV, zTLC, zRV/TL, zFRC</i>			<i>zFEV1, zFVC, zFEF25-75, zFEV1/FVC</i>			<i>zRaw, zsRaw, zsReff</i>		
	<i>Score 1</i>	<i>Score 2</i>	<i>Score 3</i>	<i>Score 1</i>	<i>Score 2</i>	<i>Score 3</i>	<i>Score 1</i>	<i>Score 2</i>	<i>Score 3</i>
<i>Score 1</i>	82.3 ± 0.10	15.1 ± 0.17	2.6 ± 0.20	40 ± 0.13	40 ± 0.34	20 ± 0.15	46 ± 0.26	48 ± 0.28	6 ± 0.9
<i>Score 2</i>	9 ± 0.13	79.1 ± 0.18	11.9 ± 0.56	48 ± 0.08	42 ± 0.23	10 ± 0.15	40 ± 0.22	22.5 ± 0.18	37.5 ± 0.19
<i>Score 3</i>	8 ± 0.15	10 ± 0.20	82 ± 0.13	30 ± 0.13	40 ± 0.26	30 ± 0.28	37 ± 0.18	38 ± 0.56	25 ± 0.29
<i>Atelectasis</i>									
	<i>zRV, zTLC, zRV/TL, zFRC</i>			<i>zFEV1, zFVC, zFEF25-75, zFEV1/FVC</i>			<i>zRaw, zsRaw, zsReff</i>		
	<i>Score 1</i>	<i>Score 2</i>	<i>Score 3</i>	<i>Score 1</i>	<i>Score 2</i>	<i>Score 3</i>	<i>Score 1</i>	<i>Score 2</i>	<i>Score 3</i>
<i>Score-1</i>	69.6 ± 0.21	18.9 ± 0.18	11.5 ± 0.13	32 ± 0.46	25.7 ± 0.33	42.3 ± 0.31	20.1 ± 0.12	46.33 ± 0.22	33.6 ± 0.36
<i>Score 2</i>	27 ± 0.3	64.6 ± 0.21	8.4 ± 0.12	26 ± 0.24	30 ± 0.26	44 ± 0.16	27.67 ± 0.11	26.33 ± 0.68	45.0 ± 0.17
<i>Score 3</i>	10.3 ± 0.22	15.9 ± 0.3	73.8 ± 0.14	40.2 ± 0.53	20 ± 0.15	39.8 ± 0.56	50 ± 0.24	19 ± 0.11	31 ± 0.21
<i>Extension of Bronchiectasis</i>									
	<i>zRV, zTLC, zRV/TL, zFRC</i>			<i>zFEV1, zFVC, zFEF25-75, zFEV1/FVC</i>			<i>zRaw, zsRaw, zsReff</i>		
	<i>Score 1</i>	<i>Score 2</i>	<i>Score 3</i>	<i>Score 1</i>	<i>Score 2</i>	<i>Score 3</i>	<i>Score 1</i>	<i>Score 2</i>	<i>Score 3</i>
<i>Score 1</i>	75 ± 0.18	21.6 ± 0.15	3.3 ± 0.7	34.2 ± 0.24	50 ± 0.28	15.71 ± 0.23	36.6 ± 0.25	50 ± 0.22	13.3 ± 0.17
<i>Score 2</i>	19.6 ± 0.10	60.4 ± 0.10	20 ± 0.10	53.33 ± 0.26	40 ± 0.21	6.66 ± 0.17	50 ± 0.32	33.3 ± 0.22	16.6 ± 0.23
<i>Score 3</i>	10 ± 0.42	10 ± 0.31	80 ± 0.24	40 ± 0.48	30 ± 0.51	30 ± 0.48	20 ± 0.42	30 ± 0.48	50 ± 0.52
<i>Total Score</i>									
	<i>zRV, zTLC, zRV/TL, zFRC</i>			<i>zFEV1, zFVC, zFEF25-75, zFEV1/FVC</i>			<i>zRaw, zsRaw, zsReff</i>		
	<i>Score 1</i>	<i>Score 2</i>	<i>Score 3</i>	<i>Score 1</i>	<i>Score 2</i>	<i>Score 3</i>	<i>Score 1</i>	<i>Score 2</i>	<i>Score 3</i>
<i>Score 1</i>	77.1 ± 0.35	11.1 ± 0.30	10.8 ± 0.10	23 ± 0.35	53.33 ± 0.42	23.33 ± 0.27	23.3 ± 0.27	63.3 ± 0.33	13.3 ± 0.23
<i>Score 2</i>	18.6 ± 0.14	66.5 ± 0.25	14.9 ± 0.13	31.66 ± 0.16	50.00 ± 0.23	18.33.11 ± 0.19	26.5 ± 0.19	55 ± 0.23	18.33 ± 0.12
<i>Score 3</i>	5.6 ± 0.37	8 ± 0.13	86.4 ± 0.29	15 ± 0.24	40 ± 0.31	45 ± 0.36	25 ± 0.35	40 ± 0.39	35 ± 0.33

Table 1. Models based on body plethysmography, spirometry, or parameters of airway mechanics (Raw, sRaw and sReff) (expressed as z scores) and correct recognition (expressed as mean ± standard deviation) of focal air-trapping and atelectasis severity, extension of bronchiectasis, and total lung impairment on chest HRCT, respectively.